**Naval Research Laboratory**
Washington, DC 20375-5320

NRL/MR/6793--93-7373



# Designs for a 10.6 μm Electromagnetic Wiggler Free-Electron Laser (FEL)

ARNE W. FLIFLET
WALLACE M. MANHEIMER

*Beam Physics Branch*
*Plasma Physics Division*



August 30, 1993

# REPORT DOCUMENTATION PAGE

*Form Approved*
*OMB No. 0704-0188*



| 1. AGENCY USE ONLY (*Leave Blank*) | 2. REPORT DATE | 3. REPORT TYPE AND DATES COVERED |
|---|---|---|
| | August 30, 1993 | |

**4. TITLE AND SUBTITLE**

Designs for a 10.6 μm Electromagnetic Wiggler Free-Electron Laser (FEL)

**5. FUNDING NUMBERS**

**6. AUTHOR(S).**

Arne W. Fliflet and Wallace M Manheimer

**7. PERFORMING ORGANIZATION NAME(S) AND ADDRESS(ES)**

Naval Research Laboratory
Washington, DC 20375-5320

**8. PERFORMING ORGANIZATION REPORT NUMBER**

NRL/MR/6793--93-7373

**9. SPONSORING/MONITORING AGENCY NAME(S) AND ADDRESS(ES)**

Office of Naval Research
Arlington, VA 22217

**10. SPONSORING/MONITORING AGENCY REPORT NUMBER**

**11. SUPPLEMENTARY NOTES**

**12a. DISTRIBUTION/AVAILABILITY STATEMENT**

Approved for public release; distribution unlimited.

**12b. DISTRIBUTION CODE**

**13. ABSTRACT** (*Maximum 200 words*)

The possibility of developing gyrotron-powered electromagnetic wiggler free-electron laser (FEL) oscillators is of considerable interest for reducing the electron energy required for operation in the infrared spectrum. This memorandum considers the design of a 10.6 μm electromagnetic wiggler FEL experiment based on the University of California at Santa Barbara (UCSB) 6 MeV electrostatic accelerator. Both waveguide and quasioptical wiggler resonator configurations are considered. A prescription for optimizing the gain of a waveguide electromagnetic wiggler FEL is derived and the nonlinear regime is treated by relating the electromagnetic wiggler FEL equations-of-motion to the "Universal" normalized FEL equations. Point designs are given showing accelerator, gyrotron, and output parameters for 10.6 μm Proof-of-Principle FEL experiments based on both waveguide gyrotron and quasioptical gyrotron wigglers. Designs are given for both 5 A and 2 A FEL electron beam currents.

**14. SUBJECT TERMS**

Gyrotron-powered-wiggler
Electromagnetic wiggler
Free-electron laser
Infrared radiation
Gyrotron
Electrostatic accelerator
Quasioptical gyrotron

**15. NUMBER OF PAGES**

29

**16. PRICE CODE**

| 17. SECURITY CLASSIFICATION OF REPORT | 18. SECURITY CLASSIFICATION OF THIS PAGE | 19. SECURITY CLASSIFICATION OF ABSTRACT | 20. LIMITATION OF ABSTRACT |
|---|---|---|---|
| UNCLASSIFIED | UNCLASSIFIED | UNCLASSIFIED | UL |

NSN 7540-01-280-5500

Standard Form 298 (Rev. 2-89)
Prescribed by ANSI Std 239-18
298-102

## CONTENTS


I. Introduction . . . . . 1

II. Design of Waveguide-Gyrotron-Wiggler FELs . . . . . 2

II-A Theory of the Low-Gain FEL Oscillator . . . . . 3
II-B FEL Electron Beam Quality Requirements . . . . . 8
II-C Gyrotron-Powered Waveguide Wiggler Fields . . . . . 9
II-D Gyrotron-Wiggler Resonator Ohmic Q . . . . . 12
II-E Electron Gun for WG-Wiggler . . . . . 12

III. Electromagnetic Wiggler FEL Point Designs . . . . . 14

III-A WG-Wiggler FEL . . . . . 14
III-B QOG-Wiggler FEL . . . . . 17

IV. Discussion of the WG-and QOG-Wiggler FEL Designs . . . . . 17

V. Acknowledgements . . . . . 21

References . . . . . 21

**DESIGNS FOR A 10.6 $\mu$m ELECTROMAGNETIC WIGGLER FREE-ELECTRON (FEL)**

# I Introduction

There is currently considerable interest in compact, tunable radiation sources capable of operating in the vibrational infrared (IR) (3—30$\mu$m)[1]. Free-electron lasers (FELs) capable of operating in this regime have been developed over the years at a small number of fixed facilities around the United States and the world. Wider use of FELs is currently inhibited by system size, cost, and shielding requirements. For instance, to achieve lasing in the infrared, electron beam energies of order 15—45 MeV are typically used.

The concept of an electromagnetic wiggler was introduced during the early work on FELs. The process of stimulated scattering with large energy exchange of a laser beam by a relativistic electron beam was studied by Pantell[2]. The concept of a two-stage FEL in which the first stage provides the wiggler fields for the second stage and the same electron beam is used to drive both stages was presented by Sprangle and Smith[3], by Elias[4], and by Pasour *et al.*[5]. A microwave wiggler FEL was investigated experimentally by Granatstein et al.[6]. A visible wavelength FEL with a wave guided $CO_2$ laser pump was investigated by Gover, Tang and Sprangle[7]. The design of a soft x-ray FEL with a laser-powered wiggler was treated by Gea-Banacloche et al.[8], who also considered the design of a compact infrared FEL with a microwave wiggler[9]. The use of waveguide gyrotron (WG) powered wigglers was considered by Danly et al.[10,11] and experimental results for a gyrotron-powered wiggler were obtained by Chu *et al.*[12]. The gyrotron is particularly well suited for use as a wiggler because of its ability to operate at short wavelengths with high efficiency, high circulating power, and long pulse lengths. Electrostatic (ES) linacs operating at a few MeV can be quite compact and their beam properties are well-matched to the EM wiggler. The ES linac can produce beams with very low energy spread and emittance. Long pulse lengths (up to DC) are possible by achieving near total charge recirculation. Recirculation of the electron beam has the additional benefit of greatly reducing the amount of x-ray shielding needed.

This paper discusses point designs for a 10.6 $\mu$m gyrotron-powered electromagnetic wiggler FEL experiment using an ES linac. Both WG and quasioptical gyrotron (QOG) wiggler

Manuscript approved July 2, 1993.

configurations are considered. The objective is to define credible experiments based as much as possible on existing hardware and which could be carried out relatively quickly. The operating wavelength was chosen to enable the use of a $CO_2$ laser to provide seed radiation to accclerate the start-up process, and because very low-loss ar coated mirrors are available. Moreover, 10.6 $\mu$m lies in an atmospheric window which is important for Navy applications. The design approach and design equations for the QOG-wiggler FEL have been given in previous work[15,16,17]; therefore the design equations presented here are mainly for the WG-wiggler configuration. The WG-wiggler analysis presented here is similar to the MIT work on WG-wigglers except that we consider linearly polarized radiation fields. In addition, the present work includes a nonlinear analysis of the electromagnetic wiggler FEL. This allows the FEL saturation power and output coupling to be estimated. The remainder of this paper is organized as follows: Section II discusses the theory and design principles for the WG-wiggler FEL, Section III gives electromagnetic wiggler FEL point designs based on waveguide and quasioptical gyrotrons and the UCSB FEL beamline, and Section IV presents a discussion of parameter trade-offs.

# II Design of Waveguide-Gyrotron-Wiggler FELs

This section discusses the theory and design of IR FEL oscillators based on an electromagnetic wiggler powered by a waveguide cavity gyrotron. The wiggler fields are assumed to form a $TE_{1n}$ mode in a section of cylindrical waveguide. The system concept is illustrated in Fig. 1. The design constraints for optimum single-pass gain, an important FEL figure-of-merit, are obtained, including beam quality requirements. A simple nonlinear theory is used to estimate the FEL circulating power at saturation and the required output coupling.

The theory of the low-gain electromagnetic wiggler FEL is outlined in the next subsection. Beam quality constraints are discussed in the following subsection. SI units are used in all equations unless otherwise noted.

## II-A Theory of the Low-Gain FEL Oscillator

A theory based on the Hamiltonian formalism of Kroll, Morton and Rosenbluth[18] is used to obtain the equations of motion for an FEL oscillator with an electromagnetic wiggler. The starting point is the modified Hamiltonian variational principle:

$$\delta \int_{t_1}^{t_2} (P_x \dot{x} + P_y \dot{y} + P_z \dot{z} - \mathcal{H}_0) dt = 0 \tag{1}$$

where $\mathcal{H}_0$ is the usual Hamiltonian associated with the total energy of an electron, $E$, and $P_x$, $P_y$, and $P_z$ are Cartesian components of the canonical momentum. Neglecting the electrostatic interaction between electrons, $\mathcal{H}_0$ is given by:

$$\mathcal{H}_0 \left(\vec{r}, \vec{P}, t\right) = c\sqrt{m^2c^2 + \left[\vec{P} - e\vec{A}\left(\vec{r}, t\right)\right]^2} \tag{2}$$

As we are interested in how the FEL parameters vary with $z$, it is useful to rewrite Eq.(1) as follows with $z$ as the independent variable:

$$\delta \int_{z_1}^{z_2} \left[P_x x' + P_y y' + (-E)\, t' - (-P_z)\right] dz = 0 \tag{3}$$

where derivatives with respect to $z$ are denoted by primes, $-E$ becomes the "momentum" conjugate to $t$, and $-P_z$ becomes the new Hamiltonian, i.e.,

$$\mathcal{H}_1 \left(x, P_x, y, P_y, t, -E, z\right) = -P_z \tag{4}$$

Solving Eq.(2) for $-P_z$ leads to:

$$\mathcal{H}_1 = -\left\{\left(E^2/c^2 - m^2c^2\right) - \left(P_x - eA_x\right)^2 - \left(P_y - eA_y\right)^2\right\}^{1/2} - eA_z \tag{5}$$

The wiggler and FEL vector potentials are assumed to be independent of $x, y$ in the region of the electron beam. This implies that the transverse canonical momentum $P_\perp = P_x\hat{x} + P_y\hat{y}$ is a constant of the motion; this constant is assumed to be zero, i.e., beam emittance is neglected. For linearly polarized TE or TEM mode radiation, we may set: $P_x = P_y = A_x = A_z = 0$, and the Hamiltonian takes the form:

$$\mathcal{H}_1 = -mc\left\{\gamma^2 - 1 - e^2A_y^2/m^2c^2\right\}^{1/2} \tag{6}$$

The electron beam interacts with a counter-propagating wave in the electromagnetic wiggler. The vector potential for the wiggler field can be approximated near the axis by:

$$A_{wy} = -\frac{1}{\sqrt{2}}\frac{mc}{e}a_w(z)\exp\left\{i\left(k_{||}z+\omega t\right)\right\}+\text{c.c.} \tag{7}$$

where $\omega$ is the angular frequency and $k_{||}$ is the axial wavenumber of the pump radiation, $m$ and $e$ are the electron rest mass and charge magnitude, $c$ is the speed of light, and $a_w(z)$ is the root-mean-square (rms) wiggler parameter. The wiggler parameter may have a weak $z$-dependence if the wiggler field corresponds to a Gaussian mode or is guided by a nonuniform waveguide, however, when $a_w(z) \ll 1$ there is virtually no effect on the resonant energy and thus no tapering effect. The FEL interaction generates a wave moving in the direction of the electron beam. The vector potential for this copropagating wave, which is assumed to be a Gaussian mode of an open Fabry-Perot resonator, has the form:

$$A_{sy} = \frac{1}{\sqrt{2}}\frac{mc}{e}a_s(z)\exp\left\{-\left(k_s z-\omega_s t\right)\right\}+\text{c.c.} \tag{8}$$

where

$$a_s(z) = a_{s0}\frac{w_{s0}}{w_s(z)} = \frac{a_{s0}}{\sqrt{1+\left(\frac{z}{z_0}\right)^2}}, \tag{9}$$

$w_{s0}$ is the beam waist radius of the FEL mode, and $z_0$ is the Rayleigh length. As is well known, the FEL bunching mechanism results from a "ponderomotive potential" which in the case of an electromagnetic wiggler moves at the resonant velocity:

$$v_{||r} = \frac{\omega_s-\omega}{k_s+k_{||}} \tag{10}$$

Thus it is useful to express the electron motion in terms of the slow-time-scale phase parameter $\psi = \left(k_s+k_{||}\right)z+\left(\omega_s-\omega\right)t$. Averaging over a wiggler field time period and neglecting higher harmonic interactions, the Hamiltonian $\mathcal{H}_1$ can be written in the slow-time-scale approximation as:

$$\bar{\mathcal{H}}_1 = -mc\left\{\gamma^2-1-a_w^2-a_s^2+2a_w a_s\cos\psi\right\}^{1/2} \tag{11}$$

Hamilton's equations for the conjugate coordinates $E$ and $t$ are given by:

$$\frac{\partial\bar{\mathcal{H}}_1}{\partial(-E)} = t' \tag{12}$$

$$\frac{\partial\bar{\mathcal{H}}_1}{\partial t} = -(-E') \tag{13}$$

It is convenient to express the motion in terms of $\gamma$ and $\psi$ instead of $E$ and $t$. Using the definitions of $\gamma$ and $\psi$ and Hamilton's equations one readily obtains:

$$\psi' = k_s + k_{||} + \frac{\omega_s - \omega}{mc^2}\frac{\partial \bar{\mathcal{H}}_1}{\partial \gamma} \tag{14}$$

$$\gamma' = \frac{1}{mc^2}\frac{\partial \bar{\mathcal{H}}_1}{\partial t} \tag{15}$$

Evaluating the derivatives leads to:

$$\frac{\partial \psi}{\partial z} = k_s + k_{||} - \frac{\omega_s - \omega}{c}\frac{\gamma}{\left\{\gamma^2 - 1 - a_w^2 - a_s^2 + 2a_w a_s \cos\psi\right\}^{1/2}} \tag{16}$$

$$\frac{\partial \gamma}{\partial z} = -\frac{\omega_s - \omega}{c}\frac{a_w a_s \sin\psi}{\left\{\gamma^2 - 1 - a_w^2 - a_s^2 + 2a_w a_s \cos\psi\right\}^{1/2}} \tag{17}$$

Assuming the low gain limit with $a_s \ll a_w \ll 1 \ll \gamma$, the above equations can be simplified by writing $\gamma = \gamma_r + \Delta\gamma$ where $\gamma_r$ corresponds to the resonant velocity defined by Eq.(10) to obtain:

$$\frac{\partial \psi}{\partial z} = \frac{k_s - k}{\left(\gamma_r \beta_{||r}\right)^3}\Delta\gamma \tag{18}$$

$$\frac{\partial \gamma}{\partial z} = -\frac{k_s - k}{\gamma_r \beta_{||r}} a_w a_s \sin\psi \tag{19}$$

where $k = \omega/c$ is the wavenumber of the wiggler radiation and, for a relativistic beam,

$$\gamma_r \approx \sqrt{\lambda / \left(1 + k_{||}/k\right)\lambda_s}. \tag{20}$$

It is convenient to introduce the normalized ponderomotive potential amplitude and normalized energy/detuning parameter according to:

$$\mathcal{A}(\zeta) = \frac{L^2\left(k_s - k\right)^2}{\left(\gamma_r \beta_{||r}\right)^4}\frac{a_w a_{s0}}{\sqrt{1 + 4\zeta^2}} \tag{21}$$

$$\mathcal{P} = \frac{L\left(k_s - k\right)}{\left(\gamma_r \beta_{||r}\right)^3}\Delta\gamma \tag{22}$$

where $\zeta = z/L$, $L = 2z_0$ is the interaction length, and a uniform wiggler field has been assumed. With these definitions, the FEL equations of motion can be expressed in the following simple form[19]:

$$\frac{d\mathcal{P}}{d\zeta} = -\mathcal{A}(\zeta)\sin\psi \tag{23}$$

$$\frac{d\psi}{d\zeta} = \mathcal{P} \tag{24}$$

These equations may be further simplified by replacing $\mathcal{A}(\zeta)$ by its value averaged over the interaction region $(-1/2 < \zeta < 1/2)$:

$$\bar{\mathcal{A}} = \sqrt{\frac{\pi}{4}} \frac{L^2 (k_s - k)^2}{\left(\gamma_r \beta_{\|r}\right)^4} a_w a_{s0} \tag{25}$$

The use of the average ponderomative potential amplitude is justified when the wiggler parameter is small. In this approximation Eqs.(23) and (24) apply to a constant wiggler, low-gain FEL and have been solved numerically by Booske et al. [20]. The solutions depend on $\bar{\mathcal{A}}$ and the initial detuning $\mathcal{P}_{inj}$ and can be displayed as a contour plot as shown in Fig. 2. The figure shows contours of constant normalized efficiency $\Delta\mathcal{P} \equiv \mathcal{P}_{inj} - \langle \mathcal{P}(1/2) \rangle$ where $\langle\ \rangle$ denotes an average over the phase $\psi(\zeta = -1/2)$. The electronic efficiency of the FEL is then given by:

$$\eta = \frac{c}{L(\omega_s - \omega)} \frac{\left(\gamma_r \beta_{\|r}\right)^3}{\gamma_{inj} - 1} \Delta\mathcal{P} \approx \frac{\Delta\mathcal{P}}{4\pi N} \tag{26}$$

The last expression is obtained by assuming $\gamma_{inj} \gg 1$ and $\omega_s \gg \omega$, and yields the usual FEL saturation efficiency estimate when $\Delta\mathcal{P} \sim 2\pi$. Eqs.(23) and (24) can be solved in the linear regime to obtain the normalized small-signal efficiency:

$$\Delta\mathcal{P}_{ss} = -\frac{\bar{\mathcal{A}}^2}{4} \frac{\mathrm{d}}{\mathrm{d}\mathcal{P}_{inj}} \left( \frac{\sin(\mathcal{P}_{inj}/2)}{\mathcal{P}_{inj}/2} \right)^2 \tag{27}$$

The rms circulating power in a $TE_{1n}$ mode of the wiggler (see below) and the Gaussian FEL radiation mode are given by:

$$P_w = 4P_0 \left(x_{1n}^2 - 1\right) J_{1n}^2 (x_{1n}) \frac{k k_{\|}}{k_\perp^2} a_w^2, \tag{28}$$

$$P_s = 4\pi^2 P_0 \frac{w_s^2}{\lambda_s^2} a_s^2, \tag{29}$$

where $P_0 = \pi m^2 c^4/(2e^2 Z_0) = 1.09$ GW. It follows that the small-signal power gain per pass, $G = \Delta P_s/P_s$, for a FEL with a cold filamentary electron beam in the low-gain Compton regime is given by:

$$G^{(c)} = -\frac{1}{16} \frac{I}{I_A} \frac{\lambda_s^2}{\sigma_s} \frac{(k_s - k)^3 L^3}{\left(\gamma_r \beta_{\|r}\right)^5} a_w^2 \frac{\mathrm{d}}{\mathrm{d}P_{inj}} \left( \frac{\sin(P_{inj}/2)}{P_{inj}/2} \right)^2 \tag{30}$$

where $\sigma_s$ is the FEL mode area, $I$ is the electron current within the mode area, $I_A = 4\pi mc^2/(Z_0 e) \sim 17000$ A is the Alfvén current, and $Z_0 = 377$ ohms. The maximum gain is obtained for $P_{inj} \sim 2.6$ which yields

$$-\frac{d}{dP_{inj}}\left(\frac{\sin(P_{inj}/2)}{P_{inj}/2}\right)^2 \approx 0.27. \tag{31}$$

The relativistic electron beam and the wiggler wave pass through each other at essentially the same speed so that the number of wave periods encountered by an electron passing through the wiggler is given by:

$$N = \frac{2L}{\lambda_p}. \tag{32}$$

For a relativistic beam the peak gain is given in terms of $N$ as:

$$G^{(c)} = 2\pi^3 \frac{I}{I_A}\frac{\lambda_s^{3/2}\lambda_p^{1/2}}{\sigma_s} a_w^2 N^3 (0.27). \tag{33}$$

The minimum radiation waist of the FEL mode is determined by the required Rayleigh length. This fixes the minimum radiation waist of the FEL mode as:

$$w_s = \sqrt{\frac{L\lambda_s}{2\pi}}, \tag{34}$$

The FEL radiation beam waist constrains the maximum size of the electron beam radius consistent with low coupling losses. For the case of the lowest order Gaussian mode, the effective FEL mode area is given by: $\sigma_s = \pi w_s^2/2$[21]. Thus, to match the electron beam cross section to the effective area of the radiation beam requires: $r_b \leq w_s/\sqrt{2}$ (filling factor of 1). Using these relationships, substituting for $a_w$, and using the optimum value of $P_{inj}$, leads to the following expression for the peak cold beam gain using an electromagnetic wiggler:

$$G_{opt}^{(c)} = 16\pi^3 \sqrt{\frac{\lambda_s}{\lambda_p}\frac{I}{I_A}} a_w^2 N^2 (0.27) \tag{35}$$

The rms circulating power in the FEL resonator at saturation is given by:

$$P_s = \frac{8P_0\left(\gamma_r \beta_{\|r}\right)^8 \bar{A}^2}{(k_s - k)^4 L^3 \lambda_s a_w^2} \approx \frac{P_0 \gamma^2 \bar{A}^2}{4\pi^4 N^3 a_w^2} \tag{36}$$

In the cold beam limit, the ratio of the steady-state beam current to the minimum start current is denoted by $\chi = I/I_{start}$ and is given by:

$$\chi = \frac{\bar{A}^2}{4\Delta\mathcal{P}}\,(0.27) \tag{37}$$

Contours of constant $\chi$ are plotted in Fig. 2. Thus, the output coupling per pass coefficient (neglecting losses) required for steady-state operation at given values for $\bar{A}$ and efficiency is:

$$T = \frac{14.8\Delta\mathcal{P}G^{(c)}}{\bar{A}^2} \tag{38}$$

## II-B FEL Electron Beam Quality Requirements

The achievable electron beam quality places significant restrictions on the parameters of the FEL available for operation near the cold-beam limit. To operate near the cold beam regime, the inhomogeneous broadening associated with beam energy spread, emittance, transverse wiggler gradients, and space charge should be less than the homogeneous gain bandwith. Following the approach of Jerby and Gover[22], expressing the FEL mode area and pump mode radiation waist in terms of the number of wiggler periods, and accounting for energy spread, finite emittance, space charge, and wiggler transverse gradient detuning effects, the following expression is obtained for the warm-beam electromagnetic wiggler FEL gain[15,16]:

$$G_{em}^{(w)} = 16\pi^3\sqrt{\frac{\lambda_s}{\lambda_p}}a_w^2\frac{I}{I_A}N^2\,(0.27)\cdot\left[1+\left(2N\frac{\Delta E}{E}\right)^2+\left(\frac{16\pi\varepsilon_n^2}{\lambda_p\lambda_s}\right)^2+\left(\frac{2NI}{I_A}\right)^2+\left(Na_w^2k_\perp^2r_b^2\right)^2\right]^{-1} \tag{39}$$

The detuning spread due to energy spread is given by[22]:

$$\theta_{th,1} = 2\pi N\frac{\Delta E}{E} \tag{40}$$

The detuning due to finite emittance is given by[22]:

$$\theta_{th,2} = 2\pi N\frac{\varepsilon_n^2}{r_b^2} \tag{41}$$

where $\varepsilon_n$ is the normalized emittance. The detuning spread due to space charge is given by[22]:

$$\theta_{th,3} = 2\pi N\frac{\nu}{\gamma} \tag{42}$$

where Budker's parameter is given by: $\nu = \gamma I / I_A$. The detuning due to the transverse field inhomogeneity in a waveguide wiggler is [10]:

$$\theta_{th,4} = \pi N a_w^2 k_\perp^2 r_b^2 \tag{43}$$

For comparison, the transverse gradient detuning for a magnetostatic wiggler is given by:

$$\theta_{th,msw} = \pi N a_w^2 k_w^2 r_b^2 \tag{44}$$

where $k_w$ is the wavenumber for the magnetostatic wiggler. To avoid a large reduction in the gain from the cold beam value, each of the above detuning parameters should be less than $\pi$ radians. The detuning effect due to transverse wiggler gradients is typically very small for millimeter-wave electromagnetic wigglers.

## II-C Gyrotron-Powered Waveguide Wiggler Fields

The electric field of a TE mode backward traveling wave in a waveguide can be written in the form:

$$\vec{E} = \frac{1}{2} f^- \vec{e}_{mn}(r, \theta; z)\, e^{i\left(k_{\|} z + \omega t + \pi/2\right)} + \text{c.c.} \tag{45}$$

where $f^-$ is an amplitude factor with dimensions of voltage and $\vec{e}_{mn}$ is a transverse vector mode function which satisfies:

$$\int_A da\ \vec{e}_i \cdot \vec{e}_j = \delta_{ij}, \tag{46}$$

and may depend parametrically on $z$. For a TE mode: $\vec{e}_{mn} = \hat{z} \times \vec{\nabla}_t \psi_{mn}$ where, for a linearly polarized mode, the scalar mode function is given by

$$\psi_{mn} = C_{mn}^{\ell} J_m(k_{mn} r) \cos(m\theta) \tag{47}$$

where $C_{mn}^{\ell}$ is a normalization coefficient given by

$$C_{mn}^{\ell} = \frac{\sqrt{2}}{\sqrt{\pi (x_{mn}^2 - m^2) J_m(x_{mn})}}, \tag{48}$$

$k_{mn} = x_{mn}/r_w$, $J_m$ is a regular Bessel function, $x_{mn}$ is a zero of $J_m'$, and $r_w$ is the waveguide radius. $TE_{1n}$ modes are of particular interest for wiggler operation because these modes

have strong on-axis transverse fields, i.e.,

$$\vec{e}_{1n}(r,\theta;z) = \frac{C_{1n}^{\ell} k_{1n}}{2}\left[J_0(k_{1n}r)\,\hat{y} - J_2(k_{1n}r)\left(\cos\theta\,\hat{\theta} - \sin\theta\,\hat{r}\right)\right] \tag{49}$$

In the Coulomb gauge $\vec{E} = -\partial A/\partial t$ so that

$$\vec{A}(\vec{r}) = -\frac{1}{2}\tilde{A}^{-}\vec{e}_{mn}(\vec{r})\,e^{i\left(k_{\|}z+\omega t\right)} + \text{c.c.} \tag{50}$$

where $\tilde{A}^{-} = f^{-}/\omega$. It follows that, for a linearly-polarized FEL interaction localized near the axis, the rms wiggler parameter is given by:

$$a_w = \frac{e}{mc^2}\frac{C_{1n}^{\ell} k_{1n}}{2\sqrt{2}k} f^{-} \tag{51}$$

To estimate the wiggler fields obtainable with a waveguide gyrotron, consider a system with the wiggler and gyrotron cavities having a common axis and joined by a gradual taper to obtain strong coupling with minimal mode conversion. The gyrotron has an annular electron beam which coincides with an off-axis peak of the $TE_{1n}$ interaction mode and the gyrotron electron gun has a hollow cathode to allow the FEL radiation and electron beams to exit from the wiggler. As is well known, the nonlinear operation of the gyrotron can be expressed in terms of a few normalized parameters including the normalized rf field amplitude $F$ and interaction length $\mu$. The nonlinear equations of motion can be solved numerically and the nonlinear single-mode efficiency for optimized detuning and a given harmonic number $s$ can be displayed on an $F-\mu$ plot[23]. For circular polarization, the normalized field amplitude is the same for all beam electrons. For linear polarization the field amplitude depends on the guiding center angle $\Theta_0$ of the beam electron and the interaction must be averaged with respect to this angle to obtain the efficiency. The general expression for the guiding-center-dependent field amplitude of a $TE_{mn}$ mode is given by

$$F^{\ell}(\Theta_0) = \frac{e}{mc^2}\frac{1}{\gamma_0\beta_{\perp 0}^{4-s}}\left(\frac{s^{s-1}}{2^{s-1}s}\right)C_{mn}^{\ell}\frac{1}{2}\left[J_{m-s}(k_{mn}r_b)\,e^{-im\Theta_0} + (-1)^s J_{m+s}(k_{mn}r_b)\,e^{+im\Theta_0}\right] f \tag{52}$$

Specializing to the fundamental harmonic interaction with a linearly polarized $TE_{1n}$ mode with the annular electron located on an outer peak of the electric field leads to:

$$F^{\ell}(\Theta_0) = F\cos\Theta_0 \tag{53}$$

where

$$F = \frac{e}{mc^2}\frac{1}{\gamma_0\beta_{\perp 0}^3}C_{1n}^{\ell}J_0\left(k_{1n}r_b\right)f \tag{54}$$

and the fact that $J_2(z) = -J_0(z)$ at a peak of $J_0$ has been used. The peak field characterized by $F$ in a linearly polarized gyrotron should be comparable or somewhat higher than the peak field in a circularly polarized gyrotron but the efficiency will be $\sim 30\%$ lower due to the average over guiding centers. The gyrotron interaction mode has near-zero group velocity and involves both the forward and backward components of the longitudinal standing wave. Thus the interaction field amplitude $f = 2f_1^-$, where $f_1^-$ is the amplitude of the backward propagating mode in the gyrotron cavity. Assuming conservation of axial power flow in the combined gyrotron wiggler resonator leads to the following relation between the field amplitude in the wiggler section ($f_2^-$) and the field amplitude in the gyrotron cavity:

$$f_2^- = \sqrt{\frac{k_{\|1}}{k_{\|2}}}f_1^- \tag{55}$$

and the wiggler parameter can be expressed in terms of the normalized field in the gyrotron according to:

$$a_w = \frac{1}{4\sqrt{2}}\frac{k_{\perp 2}}{k}\sqrt{\frac{k_{\|1}}{k_{\|2}}}\frac{\gamma_0\beta_{\perp 0}^3}{J_0\left(k_{\perp 1}r_b\right)}F \tag{56}$$

Gyrotron operation in higher order $TE_{1n}$ modes generally leads to a higher wiggler parameter (and higher FEL gain), and is needed in higher frequency wigglers to provide adequate clearance for the FEL beam. A $TE_{13}$ WG–wiggler has been demonstrated by MIT[12], but a $TE_{13}$ mode results in a gyrotron cavity and electron beam which are only marginally large enough for a 10 $\mu$m FEL. The $TE_{14}$ mode is a better choice for a 60—100 GHz WG–wiggler, but this mode is suppressed by the $TE_{62}$ mode in a circular waveguide even if slots are used. Theory indicates that the $TE_{14}$ mode can be the dominant mode in a slotted slightly noncircular waveguide[24], but this has not yet been demonstrated experimentally. The use of WG–wigglers having the present configuration above 100 GHz will probably require still higher order $TE_{1n}$ modes, whose stability has yet to be investigated.

## II-D Gyrotron-Wiggler Resonator Ohmic $Q$

The stored energy in the gyrotron-wiggler resonator can be estimated by approximating the resonator as two sections of cylindrical waveguide. This gives:

$$W = \frac{2P_w}{c}\left\{\frac{L_1 k}{k_{\|1}} + \frac{L_2 k}{k_{\|2}}\right\} \tag{57}$$

where the subscript "1" denotes the gyrotron cavity section, "2" denotes the wiggler section of the waveguide, and $k_{\|1} = \pi/L_1$. The wiggler circulating power is denoted by $P_w = (k_{\|}/2Z_0 k)|f^-|^2$. Similarly, the resonator ohmic losses are given by:

$$P_o = \frac{2}{\sigma\delta Z_0^2}\frac{x_{mn}^2}{x_{mn}^2 - m^2}\left\{\frac{L_1 k}{r_{w1}k_{\|1}}\left[\left(\frac{k_{\|1}m}{kx_{mn}}\right)^2 + \left(\frac{k_{\perp 1}}{k}\right)^2\right] + \frac{L_2 k}{r_{w2}k_{\|2}}\left[\left(\frac{k_{\|2}m}{kx_{mn}}\right)^2 + \left(\frac{k_{\perp 2}}{k}\right)^2\right]\right\} \tag{58}$$

Combining these expressions leads to a formula for the Ohmic $Q$ factor:

$$Q_o = \frac{\sigma\delta Z_0 k}{2}\frac{\left(1 - \frac{m^2}{x_{mn}^2}\right)\left[\frac{L_1 k}{k_{\|1}} + \frac{L_2 k}{k_{\|2}}\right]}{\left\{\frac{L_1 k}{r_{w1}k_{\|1}}\left[\left(\frac{k_{\|1}m}{kx_{mn}^2}\right)^2 + \left(\frac{k_{\perp 1}}{k}\right)^2\right] + \frac{L_2 k}{r_{w2}k_{\|2}}\left[\left(\frac{k_{\|2}m}{kx_{mn}^2}\right)^2 + \left(\frac{k_{\perp 2}}{k}\right)^2\right]\right\}} \tag{59}$$

## II-E Electron Gun for WG–Wiggler

In the present in-line configuration, the gyrotron electron gun has a hollow cathode to allow the FEL radiation beam and recirculating electron beam to exit the wiggler. To minimize development costs, it will be advantageous to modify an existing electron gun design. The cathode radius should be sufficiently large that the presence of the hole has little effect on the accelerating fields near the cathode experienced by the gyrotron electron beam. The gun should also be able to operate at or above 100 kV as the wiggler parameter obtainable in a given mode scales with voltage.

The present design is based on the Varian VUW-8144 electron gun which was designed for an experimental 140 GHz, $TE_{15,2}$ mode gyrotron capable of $\approx$ 1 MW output power[25]. This gun has achieved voltages above 100 kV, and currents over 50 A, during pulsed operation. The radius of the emitting surface of the cathode is 2.9 cm, thus the cathode should easily accommodate a 0.75 cm radius hole on axis. The VUW-8144 gun has an intermediate voltage "mod-anode," which allows considerable flexibility to adjust the gyrotron

| | Original | WG-Wiggler |
|---|---|---|
| TE Mode Indicies | 15,2 | 1,4 |
| Wavelength | 2.1 mm | 5 mm |
| Gyrotron cavity radius ($r_{w1}$) | 7.8 mm | 9.6 mm |
| Cavity beam radius ($r_b$) | 5.5 mm | 5.8 mm |
| Magnetic compression ratio | 28 | 25 |

Table 1: Comparison of electron beam and cavity parameters of MIT 140 GHz WG with 60 GHz WG-wiggler parameters compatible with Varian VUW-8144 electron gun.

cavity electron beam parameters by varying the cavity-to-cathode magnetic field compression ratio and the mod-anode voltage. Operating in a $TE_{14}$ (and to a greater extent, the $TE_{13}$ mode) requires a smaller electron beam than the $TE_{15,2}$ mode at a given frequency. This difference can be accommodated by increasing the magnetic compression ratio and/or decreasing the operating frequency (from 140 GHz). The maximum compression ratio is limited by loss of beam quality and the onset of beam reflection. Table 1 gives electron beam and gyrotron cavity parameters for a 60 GHz, $TE_{14}$ mode wiggler. The corresponding parameters for the VUW-8144 electron gun in the original 140 GHz gyrotron design are also given for comparison. The electron beam couples to the third peak of the cavity electric field ($r_b/r_{w1} = 0.6$). By operating at 60 GHz, the cavity beam radius and the magnetic field compression ratio are close to the original design values. Higher frequency wigglers require a higher compression ratio. For example, at 80 GHz the compression ratio must be increased to 45 to produce a smaller beam in the cavity. The feasibility of designs based on the VUW-8144 electron gun must be considered provisional until verified by trajectory calculations.

# III Electromagnetic Wiggler FEL Point Designs

## III-A WG-Wiggler FEL

The 10.6 $\mu$m WG–wiggler FEL design is based on the $TE_{14}$ mode, and a frequency of 60 GHz. A schematic of the FEL oscillator experiment is given in Fig. 1. The gyrotron cavity and wiggler waveguide sections are assumed to be slotted and to have a slightly elliptical cross section to suppress mode competition with the $TE_{62}$ mode (see Ref. [24]). The parameters of the WG–wiggler are given in Table 2. The wiggler parameter is maximized by 1) using a short gyrotron cavity to optimize the efficiency at high cavity fields, and 2) reducing the diameter of the wiggler waveguide to increase the radiation power density. A drawback to the second method is that the axial component of the wiggler field wavenumber is reduced resulting in less frequency upshift.

The accelerator parameters have been chosen to be consistent with values achieved by the UCSB FEL beam line[13], except that the current is assumed to be upgraded from 2 to 5 A. The design is based on a 600 period wiggler with an effective length of 150 cm. The FEL parameters are given in Table 3. The small signal warm beam gain per pass is 3.7% for 10 $\mu$m radiation. As indicated in the present design, the wiggler parameter $a_w$ of electromagnetic wiggler FELs will tend to be much smaller than values typical for conventional FELs, because of problems with generating high wiggler circulating powers. The small signal gain, which is proportional to the wiggler circulating power, will also usually be less than typical gains achieved by conventional FELs. The normalized ponderomotive potential was chosen to be $\bar{A} = 17$ which optimizes the the nonlinear efficiency of the FEL as shown in Fig 2. The resulting circulating power in the FEL resonator is 1.7 MW for 10.6 $\mu$m operation and the required output coupling is 1.3%. The main sources of resonance thermalization are the beam energy spread, emittance, and space-charge. There is very little detuning spread due to wiggler gradients. To estimate the useful output power, per-pass resonator losses for the ar-coated mirrors are assumed to be 0.4%, and the output coupling efficiency of a small hole in the mirror is taken to be 50%[13].

| | |
|---|---|
| Wavelength | 5 mm |
| $F$ | 0.3 |
| $\mu$ | 6.16 |
| Voltage | 100 kV |
| $\alpha = v_\perp / v_\parallel$ | 2 |
| Gyrotron Cavity Length ($L_1$) | 1 cm |
| Wiggler Cavity Length ($L_2$) | 150 cm |
| Wiggler Cavity Radius ($r_{w2}$) | 1.55 cm |
| $k_{\parallel 2}/k$ | 0.8 |
| Ohmic-$Q$ of combined resonator | 147,000 |
| Wiggler Circulating Power ($P_w$) | 5 MW |
| Wiggler Power density on-axis | 3.06 MW/cm$^2$ |
| $a_w$ | 0.0084 |
| $B_w$ | 143 G |
| Ohmic Loss Estimate | 0.8 kW |
| Diffraction Loss Estimate | 10% per pass |
| Gyrotron Output Power | 500 kW |

Table 2: Parameters of linearly polarized 60 GHz, $TE_{14}$ mode WG–wiggler.

| | |
|---|---|
| Universal FEL Amplitude ($\bar{A}$) | 17 |
| Universal FEL Efficiency ($\Delta\mathcal{P}$) | 5.4 |
| Electron Beam Energy | 5.43 MeV |
| Electron Beam Current | 5 A |
| Normalized Emittance | 10 mm mrad |
| Electron Beam Energy Spread | 1.25 keV |
| Electron Beam Diameter | 2.24 mm |
| Beam Current Density | 126 A/cm$^2$ |
| Interaction Length | 150 cm |
| FEL Radiation Waist Diameter | 3.2 mm |
| Cold Beam Gain per Pass | 4.6% |
| Warm Beam Gain per Pass | 3.8% |
| Optimum FEL Resonator Loss per Pass | 1.3% |
| FEL Saturation Power | 1.6 MW |
| FEL Interaction Efficiency | 0.08% |
| FEL Output Power | 7 kW |

Table 3: Parameters of 10.6 $\mu$m FEL based on the 60 GHz, $TE_{14}$ mode, 600 period WG-wiggler and the (upgraded) UCSB FEL beam-line.

## III-B QOG-Wiggler FEL

Design parameters have been obtained for a QOG–wiggler FEL oscillator operating at 10.6 $\mu$m. The system concept is illustrated in Figure 3. The wiggler field would be provided by a high voltage (HV) QOG operating at 95 GHz. Operation at high voltage is one way to achieve the high circulating power needed adequate single-pass gain[15]. In addition, high output power is needed to overcome losses due to wiggler mirror apertures. These losses are estimated to be $\sim$ 8% per pass for a 10 $\mu$m FEL with an 85 GHz QOG–wiggler[26]. The QOG required by the wiggler could be developed from the current experimental NRL 100 kV QOG by replacing the existing Varian VUW-8144 electron gun by the much larger and higher power Varian VUW-8101 electron gun. This gun, originally designed to produce a 500 kV, 150 A beam with $\alpha = v_\perp/v_\parallel \approx 0.5$ for high power CARM experiments[27], can also produce a high $\alpha$ ($> 1$) gyrotron beam at voltages up to 250 kV. The radius of the cathode emitting surface is 3 cm which is close to that of the VUW-8144 gun, thus a similar sized beam would be produced in the QOG resonator. The QOG–wiggler parameters are listed in Table 4. The required FEL beam energy is 3.9 MeV. The parameters of the ES linac FEL are the same as for the WG–wiggler system, except that the beam energy is lower due to the shorter wiggler wavelength. The FEL design parameters are listed in Table 5. The design is based on a 600 period wiggler with an effective length (equal to two Rayleigh lengths) of 96 cm. The wiggler circulating power is 90 MW and the average wiggler parameter is $a_w = 0.005$. The small signal warm beam gain is 2% for generation of 10.6 $\mu$m radiation. The estimated peak output power at 10.6 $\mu$m is 3.8 kW accounting for resonator losses and output coupling efficiency.

# IV Discussion of the WG– and QOG–Wiggler FEL Designs

The designs given in the previous section show that, compared to the QOG–wiggler, the WG–wiggler requires much less circulating power to achieve a given $a_w$ and single-pass gain. For comparable per-pass wiggler losses, this translates into much lower prime power required

| | |
|---|---|
| Wavelength | 3.2 mm |
| Harmonic Number | 1 |
| $f$ | 0.14 |
| $\mu$ | 14 |
| Voltage | 250 kV |
| $\alpha = v_\perp/v_\parallel$ | 1.25 |
| Beam Current | 138 A |
| Magnetic Field | 49 kG |
| Wiggler Circulating Power | 89 MW |
| Wiggler Radiation Waist Diameter | 2 cm |
| On-axis Power Density | 11.6 MW/cm$^2$ |
| $a_w$ | 0.0066 |
| $B_w$ | 220 G |
| Diffraction Loss per Pass | 8% |
| Ohmic loss | 144 kW |
| Output Power | 7.2 MW |
| Electronic Efficiency | 21% |

Table 4: Parameters of the 95 GHz QOG–wiggler.

| | |
|---|---|
| Universal FEL Amplitude ($\bar{A}$) | 17 |
| Universal FEL Efficiency ($\Delta\mathcal{P}$) | 5.4 |
| Electron Beam Energy | 3.95 MeV |
| Electron Beam Current | 5 A |
| Normalized Emittance | 10 mm mrad |
| Electron Beam Energy Spread | 1.25 keV |
| Electron Beam Diameter | 1.8 mm |
| Beam Current Density | 197 A/cm$^2$ |
| Interaction Length | 96 cm |
| FEL Radiation Waist Diameter | 2.54 mm |
| Cold Beam Gain per Pass | 2.8% |
| Warm Beam Gain per Pass | 2.2% |
| Optimum FEL Resonator Loss per Pass | 0.8% |
| FEL Saturation Power | 2.2 MW |
| FEL Interaction Efficiency | 0.08% |
| FEL Output Power | 3.8 kW |

Table 5: Parameters of a 10.6 $\mu$m FEL based on a 95 GHz, 600 period QOG–wiggler.

for the WG-wiggler. The WG–wiggler system derives its gain advantage in part from the ability to confine the wiggler radiation to a smaller cross section and thus achieve greater power density than the quasioptical Gaussian mode system. Moreover, the waveguide cross section is independent of the wiggler length unlike the quasioptical system where the cross section is proportional to the wiggler length. This factor leads to an optimum gain scaling for the WG–wiggler FEL proportional to $N^2$ where $N$ is the number of wiggler periods), compared to $N$ for the QOG–wiggler FEL (note that cross section of the IR mode also scales as $N$). The penalty for confining the mode in a waveguide is a reduction in $k_{||}$ which reduces the frequency upshift—a 20% effect in the design given. A more serious limitation to the WG-waveguide is the difficulty of scaling to shorter wavelengths, because the gyrotron cavity radius scales inversely with frequency for a given operating mode. This effect will probably limit in-line $TE_{14}$ WG-wigglers to frequencies below $\sim 100$ GHz. This would allow IR coverage down to $\sim 5$ $\mu$m at UCSB which has a 6 MeV beam. Frequency scaling is more favorable for the QOG–wiggler system, because of the open resonator and because efficient second harmonic operation appears feasible. As discussed in previous work[15], this should allow operation at frequencies up to 460 GHz with state-of-the-art superconducting magnets. If this can be achieved, it will be possible for an FEL to cover the 3—13 $\mu$m atmospheric windows with a 3 MeV electron beam. A 3 MV ES linac is compact enough for a portable shipboard or truck-mounted system.

The gain achievable for a given wiggler circulating power cannot be increased arbitrarily by increasing the FEL beam current or the number of wiggler periods because of space charge limitations. Rather, for a given current, usually set by the accelerator design, there is a maximum wiggler length over which coherence of the interaction can be maintained. At currents of a few Amperes, an optimum gain electromagnetic wiggler will have more wiggler periods (500—1500) than a conventional FEL, which reduces the saturated efficiency, but the millimeter-wave wiggler remains compact and is not subject to alignment errors. Moreover, coherence loss due to FEL beam energy spread is not usually a factor in ES linacs. On the other hand, the electromagnetic wiggler FEL is readily scalable to higher power and efficiency by increasing the FEL beam current. The saturated efficiency increases due the

shorter optimum wiggler length, and the system efficiency increases because the wiggler power—the major power drain in the present design—remains unchanged while the output power increases.

The FEL designs presented above are based on a 5 A electron beam which represents a 250% increase over what is currently available at UCSB. The scaling argument in the previous paragraph can be illustrated in reverse by reducing the FEL beam current in the above designs to 2 A. Most or all of the gain can be recovered by increasing the wiggler lengths: from 600 to a 1000 periods for the WG–wiggler, and from 600 to 1200 periods for the QOG–wiggler system. The resulting design parameters are given in Tables 6 and 7 below. The FEL output power is down considerably because of the lower electron beam power and the lower intrinsic efficiency of the longer wigglers. However, the gain reducing effects associated with space charge and energy spread are somewhat smaller for the 2 A beam.

In summary, design have been presented for relatively low voltage, IR FELs based on gyrotron-powered electromagnetic wiggler configurations and an ES linac. Both configurations appear capable of producing kilowatt peak powers at 10.6 $\mu$m. Each wiggler configuration has particular strengths: the WG–wiggler should achieve higher gain and have lower losses; the QOG–wiggler should scale to shorter wavelengths. The technical risk associated with each type of wiggler is similar. Therefore, the type of wiggler chosen for an initial experiment will largely depend on available equipment.

# V Acknowledgments

The authors gratefully acknowledge helpful discussions with Drs. P. Sprangle, S. Gold, G. Ramian, and B. Danly. This work was supported by the Office of Naval Research.

# References

[1] D. D. Dlott and M. D. Fayer, "Applications of infrared free-electron lasers: basic research on the dynamincs of molecular systems," *IEEE J. Quant. Elect.* **27**, 2697

| | |
|---|---|
| Universal FEL Amplitude ($\bar{A}$) | 17 |
| Universal FEL Efficiency ($\Delta\mathcal{P}$) | 5.4 |
| Electron Beam Energy | 5.43 MeV |
| Electron Beam Current | 2 A |
| Normalized Emittance | 10 mm mrad |
| Electron Beam Energy Spread | 0.5 keV |
| Electron Beam Diameter | 2.9 mm |
| Beam Current Density | 30 A/cm$^2$ |
| Interaction Length | 250 cm |
| FEL Radiation Waist Diameter | 4.1 mm |
| Cold Beam Gain per Pass | 5.1% |
| Warm Beam Gain per Pass | 4.6% |
| Optimum FEL Resonator Loss per Pass | 1.4% |
| FEL Saturation Power | 0.4 MW |
| FEL Interaction Efficiency | 0.047% |
| FEL Output Power | 1.8 kW |

Table 6: Parameters of 10.6 $\mu$m FEL based on the 60 GHz, $TE_{14}$ mode, 1000 period WG–wiggler and the 2 A UCSB FEL beam-line.

| | |
|---|---|
| Universal FEL Amplitude ($\bar{A}$) | 17 |
| Universal FEL Efficiency ($\Delta\mathcal{P}$) | 5.4 |
| Electron Beam Energy | 3.95 MeV |
| Electron Beam Current | 2 A |
| Normalized Emittance | 10 mm mrad |
| Electron Beam Energy Spread | 0.5 keV |
| Electron Beam Diameter | 2.5 mm |
| Beam Current Density | 39 A/cm$^2$ |
| Interaction Length | 192 cm |
| FEL Radiation Waist Diameter | 3.6 mm |
| Cold Beam Gain per Pass | 2.2% |
| Warm Beam Gain per Pass | 1.9% |
| Optimum FEL Resonator Loss per Pass | 0.62% |
| FEL Saturation Power | 0.52 MW |
| FEL Interaction Efficiency | 0.04% |
| FEL Output Power | 0.5 kW |

Table 7: Parameters of a 10.6 $\mu$m FEL based on a 95 GHz, 1200 period QOG–wiggler and the 2 A UCSB FEL beam line.

(1991).

[2] R. H. Pantell, G. Soncini, and H. E. Puthoff, "Stimulated Photon-Electron Scattering," *IEEE J. Quant. Electron.***QE-4**, 905 (1968).

[3] P. Sprangle and T. Smith, "Theory of free-electron lasers," *Phys. Rev. A***21**, 293 (1980).

[4] L. R. Elias, "High-power, cw, efficient tunable (uv through ir) free-electron laser using low-energy electron beams," *Phys. Rev.Lett.***42**, 977 (1979).

[5] J.A. Pasour, P. Sprangle, C.M. Tang, and C.A. Kapetanakos, "High-power, Two-Stage FEL Oscillator Operating in the Trapped Particle Mode," *Nucl. Instr. and Meth. in Phys. Res.***A237**, 154 (1985).

[6] V. L. Granatstein, Y. Carmel, and A. Gover,"Demonstration of a free electron laser with an electromagnetic wiggler," in *Free-Electron Generators of Coherent Radiation* SPIE Proceedings Volume 453, 344 (1983).

[7] A. Gover, C.M. Tang, and P. Sprangle, "Feasibility of D.C. to Visible High Power Conversion Employing a Stimulated Compton free-electron Laser with a Guided Wave $CO_2$ Laser Pump Wave and an axial Electric Field," *J. Appl. Phys.* **53**, 124 (1982).

[8] J. Gea-Banacloche, G. T. Moore, R. R. Schlicher, M. O. Scully, and H. Walther, "Soft x-ray free-electron laser with a laser undulator," *IEEE J. Quant. Electronics* **QE-23**, 1558 (1987).

[9] J. Gea-Banacloche, G. T. Moore, R. R. Schlicher, M. O. Scully, and H. Walther, "Proposal for a compact FEL with electromagnetic-wave undulator," *Nucl. Instr. and Meth. Phys. Res.* **272**, 199 (1988).

[10] B. G. Danly, G. Bekefi, R. C. Davidson, R. J. Temkin, T. M. Tran, and J. S. Wurtele, "Principles of gyrotron powered electromagnetic wigglers for free-electron lasers," *IEEE J. Quant. Electronics* **QE-23**, 103 (1987).

[11] T. M. Tran, B. G. Danly, and J. S. Wurtele, "Free-electron lasers with electromagnetic standing wave wigglers," *IEEE J. Quant. Electronics* **QE-23**, 1578 (1987).

[12] T.S. Chu, B.G. Danly and R. Temkin, "A gyrotron-powered standing-wave electromagnetic wiggler experiment," *Nucl. Instr. and Meth. in Phys. Res.* **285**, 246 (1989).

[13] G. Ramian, "Properties of the new UCSB free-electron lasers," *Short-Wavelength Radiation Sources*, Phillip Sprangle, Editor, Proc. SPIE 1552, 69 (1991).

[14] L.R. Elias I. Kimel, D. Larson, D. Anderson, M. Tecimer, and Z. Zhefu, "A compact cw free-electron laser," *Nucl. Instr. and Meth. in Phys. Res.* **A304**, 219 (1991).

[15] A.W. Fliflet and W.M. Manheimer, "Compact infrared long-pulse free-electron laser," NRL Formal Report 9504 (1992).

[16] A.W. Fliflet, R.P. Fischer, and W.M. Manheimer, "New results and applications for the quasioptical gyrotron," NRL Memorandum Report 7183 (1993).

[17] W.M. Manheimer and A.W. Fliflet, "Long-pulse, low-voltage infrared free-electron laser," accepted for publication in *Trans. Quant. Elect.* (1993).

[18] N.M. Kroll, P.L. Morton, and M.N. Rosenbluth, "Free-electron lasers with variable parameter wigglers," *IEEE J. Quant. Elect.* **QE-17**, 1436 (1981).

[19] J.H. Booske, A. Serbeto, T.M. Antonsen, Jr., and B. Levush, "Nonlinear analyses for optimized short-period-wiggler free-electron laser oscillators," *J. Appl. Phys.* **65**, 1453-1459 (1989).

[20] J.H. Booske, V.L. Granatstein, T.M. Antonsen, Jr., W.W. Destler, J. Finn, P.E. Latham, and B. Levush, I.D. Mayergoyz, and J. Rogers, "Free-electron laser with small period wiggler and sheet electron beam: a study of the feasibility of operation at 300 GHz with 1 MW CW output power," *Nucl. Instr. Meth. Phys. Res.* **A285**, 92-96 (1989).

[21] A. Gover, H. Freund, V. L. Granatstein, J. H. McAdoo, "Basic design considerations for FELs driven by electron beams from RF accelerators," *Infrared and Millimeter Waves*, vol. 11, Ch. 8, K. J. Button, Ed. (New York:Academic), (1984).

[22] E. Jerby and A. Gover, "Investigation of the gain regimes and gain parameters of the free-electron laser dispersion equation," *IEEE J. Quant. Electronics* **QE-21**, 1041 (1985).

[23] B.G. Danly and R.J. Temkin, *Phys. Fluids* **29**, 561 (1986).

[24] S.W. McDonald, J.M. Finn, M.E. Read, and W.M. Manheimer, "Boundary integral method, for computing eigenfunctions in slotted gyrotron cavities of arbitrary cross sections," *Int. J. Electron.* **61**, 795 (1986).

[25] H. Huey, N. Lopez, R. Garcia, and K.E. Kreischer, "A magnetron injection gun for the MIT Megawatt gyrotron," *Digest of the Tenth Int. Conf. on IR and MM Waves*, Lake Buena Vista, FL, Dec. 9—13, 1985 (R.J. Temkin, Ed.).

[26] G. Ramian, private communication (February, 1993).

[27] R.B. McCowan, R.A. Pendleton, and A.W. Fliflet, "Design of an electron gun for a 280 GHz induced-resonance-electron-cyclotron (IREC) maser experiment," *Trans. Elect. Dev.* **39**, 1763 (1992).

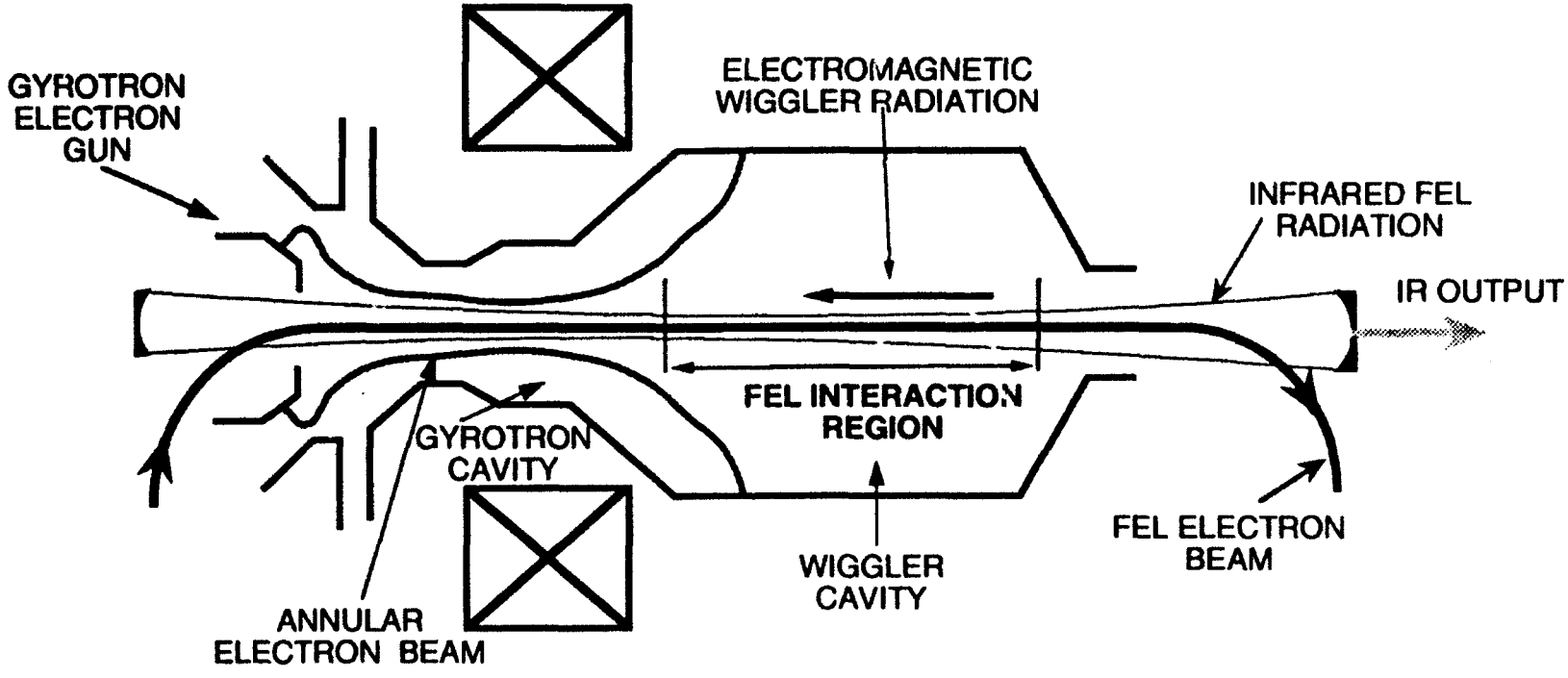


Figure 1. Schematic of an IR FEL with a WG-wiggler showing the FEL beam path and interaction region, waveguide gyrotron-wiggler resonator, and IR FEL resonator.

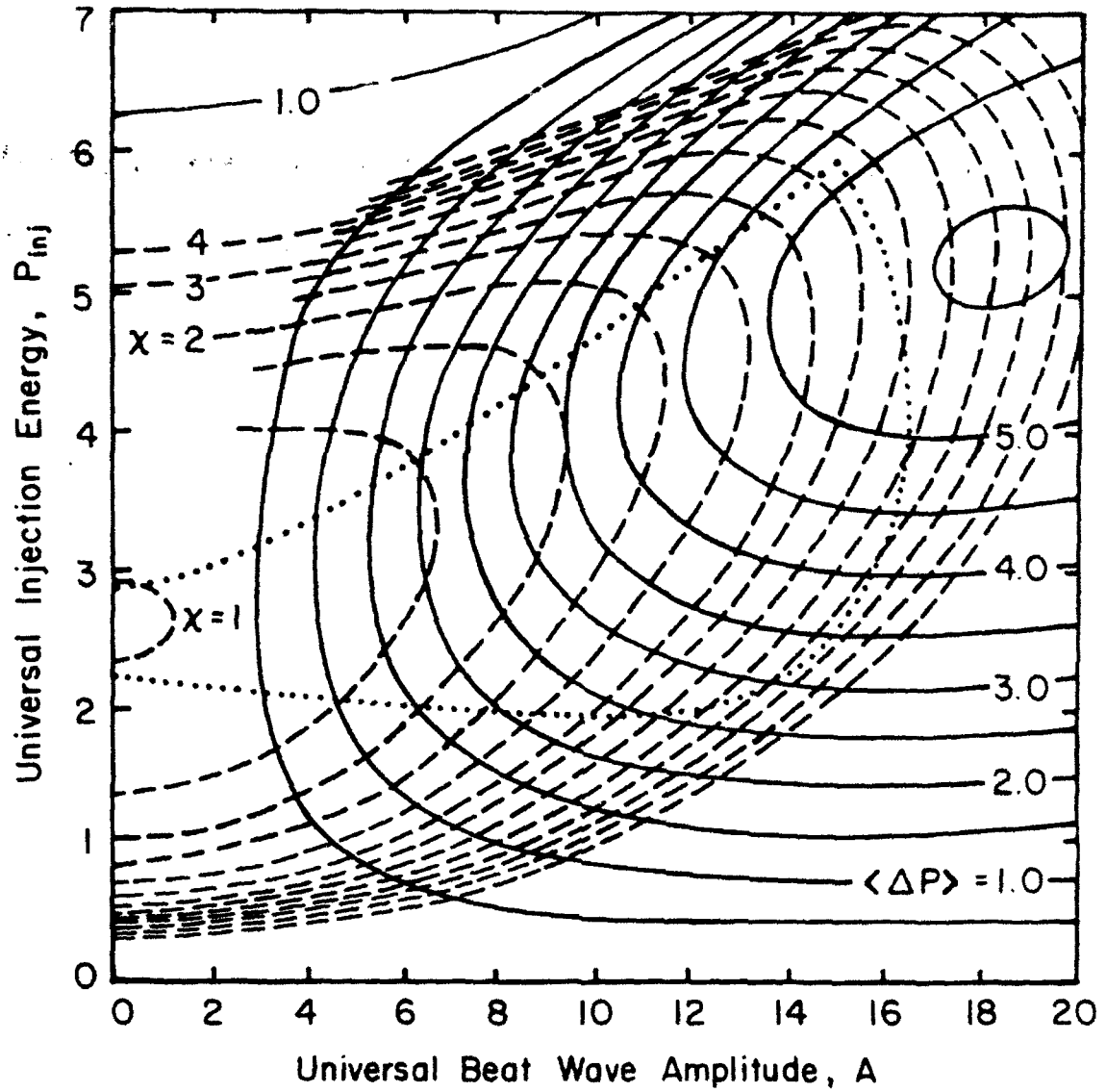


**Figure 2.** FEL oscillator universal operating map[20]. The solid lines are contours of constant $\Delta\mathcal{P}$. The dashed lines represent equilibrium states parameterized by constant $\chi$, the ratio of beam current to the minimum start current. The region of stable single-mode equilibria is bounded by the dotted line. The average beat-wave amplitude $\bar{A}$ is denoted by $A$ in the figure. ©1989 North Holland.

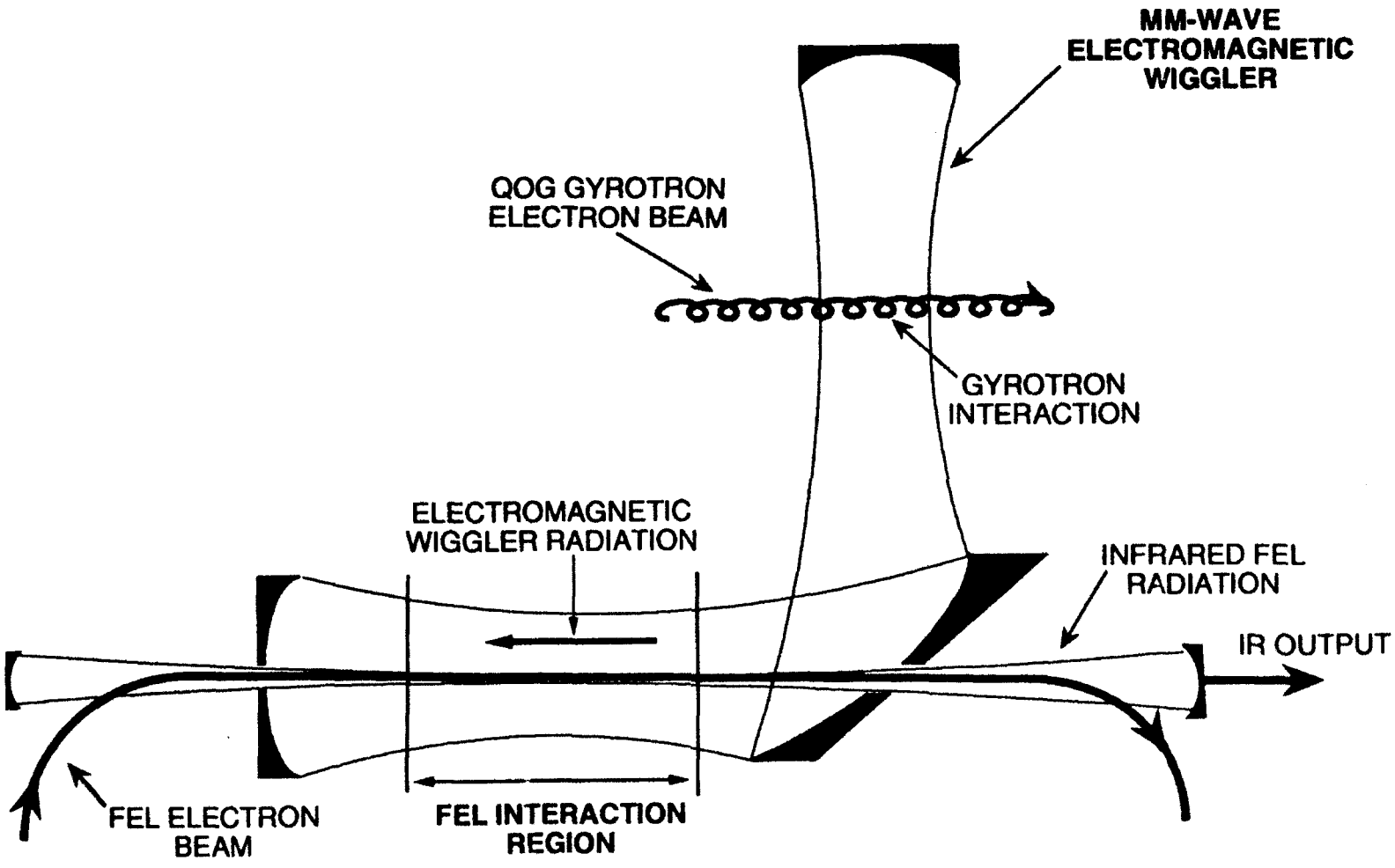


Figure 3. Schematic of an IR FEL with a QOG-pumped electromagnetic wiggler showing the FEL beam path and interaction region, sub-millimeter-wave QOG-wiggler resonator, and IR FEL resonator.